Supporting Information

The signaling properties of a signal transduction covalent modification cycle are altered by a downstream target

Alejandra C. Ventura, Peng Jiang, Lauren Van Wassenhove, Domitilla Del Vecchio, Sofia D. Merajver, and Alexander J. Ninfa

Contents

A. Supporting Experiments

(1) Kinetics of the UTase/UR-PII monocycle.

(2) Complexes formed between NRII and partially-modified PII trimers.

(3) Forming heterotrimeric PII proteins *in vitro*.

(4) Inhibition of the UT activity of the UTase/UR by NRII was lost when high concentrations of PII were present.

(5) Residual UT activity in the presence of glutamine.

(6) Biphasic effects of NRII on PII uridylylation were still observed at 2 μM NRII

B. Calculation of n_H and S_{50}

C. A simple model allowing analytical solutions

D. A detailed kinetic model for the UTase/UR-PII cycle and the effects of NRII

(1) Model description.

(2) Schemes representing the model.

(3) Model parameters.

(4) Predictions of the model.

(5) Model equations.

E. Supporting Information References

A. Supporting Experiments

(1) Kinetics of the UTase/UR-PII monocycle.

Under the conditions of our experiments, the reconstituted UTase/UR-PII cycle attained the steady state level of PII modification within several minutes (Fig S1A). Control experiments showed that upon perturbation of the glutamine concentration, the reconstituted system could

rapidly attain the new steady state position, indicating that both UT and UR activities were operating as expected (Fig S1B).

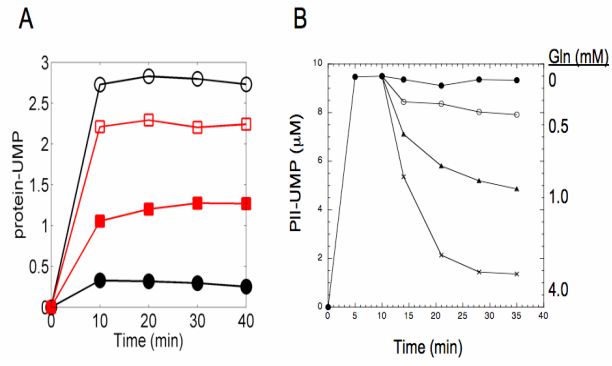

Figure S1. The UTase/UR-PII monocycle attained the steady state level of PII modification within minutes. (A). Time courses for PII modification in the presence or absence of NRII. Reaction conditions were as in Materials and Methods. ○ and □, 0.1 mM glutamine;● and ■, 2 mM glutamine; circles correspond to no NRII, squares to 10 μM NRII. **(B). The system rapidly achieved a new steady state upon perturbation with glutamine.** Reaction conditions were as in Materials and Methods, and contained wild-type PII at 3 μM and 0.6 μM UTase/UR. The reaction mixture initially lacked glutamine, and as shown, within 10 min PII was fully uridylylated. At 10 min, the reaction was split into aliquots, and glutamine was added as indicated. As shown, the system then attained a new steady state reflecting the increased glutamine concentration.

(2) Complexes formed between NRII and partially-modified PII trimers

PII forms a homotrimer that resembles a squat barrel with three large "T" loops extending from one side (reviewed in ref S1 and S2). The T loops are the portion of the protein that interacts with the PII receptor proteins, such as NRII, and contain the Y51 residue that is the site of uridylylation. Since PII is trimeric, it may contain from zero to three covalently attached uridylyl groups. Studies with purified components indicated that the modification and de-modification of PII by the UTase/UR was non-processive and non-cooperative (independent of the status of the other subunits in the PII trimer). As PII became modified and de-modified *in vitro*, the partially modified species (PII trimers with one or two uridylyl-groups) were evident and present in the quantities predicted from a mechanism where each site is independently modified/de-modified (ref S3). Fully modified PII-UMP (containing modifications at all three Y51 sites in the trimer) failed to interact with NRII. Most likely, the uridylyl group interferes with the binding of the T-loop by NRII. In contrast, unmodified PII is a potent regulator of NRII. Prior enzymological studies of PII have focused upon the properties and activities of the

fully modified or unmodified protein, as these studies are the easiest to perform and interpret.

We provide biochemical evidence that NRII binds to partially modified PII trimers (P_1, P_2). For example, when binding of partially modifed trimers (P_1 and P_2) to NRII was studied by non-denaturing gel electrophoresis, a variety of PII-NRII complexes were detected (Fig S2).

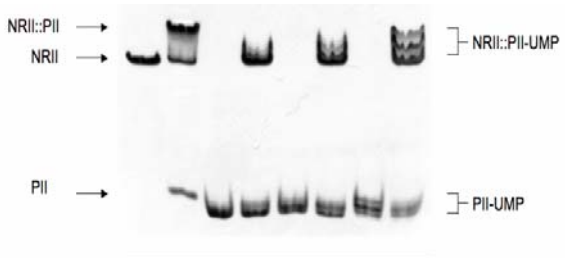

UTase/UR μM	0.5	-	0.5	0.5	0.5	0.5	0.5	0.5
NRII μM	6	6	-	6	-	6	-	6
PII μM	-	12	12	12	12	12	12	12
Gln mM	-	-	-	-	0.5	0.5	2	2

Figure S2. **Non-denaturing gel electrophoresis analysis of complexes formed between NRII and partially-modified PII trimers.** Reaction mixture conditions were as in monocycle experiments and contained glutamine as indicated to result in intermediate levels of PII uridylation. Aliquots of reaction mixtures were fractionated on non-denaturing polyacrylamide gels (ref S4). The gel was stained with Commassie Brilliant Blue R-250 and photographed with trans-illumination. In additional experiments, we utilized α-[^{32}P]-UTP to label partially-modified PII trimers, and observed that the species indicated here as NRII::PII-UMP were indeed labeled with ^{32}P.

(3) Forming heterotrimeric PII proteins *in vitro*.

We previously described conditions under which the subunits of the trimeric PII protein could be reversibly dissociated by addition and removal of urea, and we identified a mutant form of PII bearing a 7-amino acid truncation at the apex of the T-loop that formed trimers normally, bound small molecule effectors normally, and displayed normal subunit interactions, yet failed to bind to any of the PII receptor proteins (ref S5, 12). This allowed the formation of heterotrimeric, monovalent, forms of PII *in vitro* from wild-type and mutant subunits (12). Here, we use this heterotrimeric, monovalent, form of PII as a reagent to create a simplified system to measure retroactive effects. Heterotrimers were formed using a 6-fold excess of the mutant subunits relative to wild-type subunits, and non-denaturing gel electrophoresis of PII trimers followed by Coomassie Blue staining of gels showed that in the heterotrimer PII preparation, most of the trimers contained three mutant subunits (as planned), most of the wild-type subunits were found in PII trimers that contained 2 mutant subunits ("monovalent PII"), and a small but discernable fraction of the wild-type subunits were found in trimers that had two wild-type

subunits and one mutant subunit ("divalent PII"). Surely, there was also an even smaller fraction containing three wild-type subunits ("trivalent PII"), but this was below the level of detection.

The experiments employing heterotrimeric PII described above utilized a mutant form of PII with a small deletion at the apex of its T-loop (D47-53); this mutant form of PII had been studied in some detail (refs S4, S5, 12). Nevertheless, to test whether the results obtained in Fig 2D were due to some unforeseen property of the mutant PII subunits, the experiments with heterotrimeric PII were repeated utilizing a different mutant form of PII, containing the G89A mutation (refs S4, S5, 12). We observed that a result very similar to that shown in Fig 2D was obtained when heterotrimeric PII containing wild type and G89A subunits was used (Fig S3). Thus, the results in Fig 2D appear to reflect the use of monovalent PII, rather than a unique property of the specific mutant PII subunits used to form the monovalent PII sample.

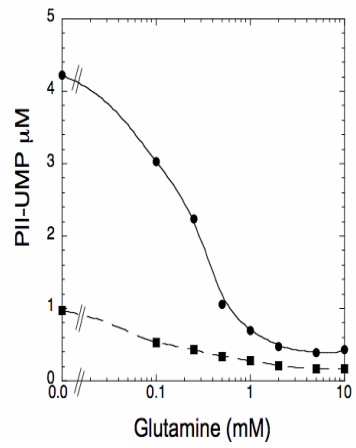

Figure S3. Effect of NRII on the steady-state level of PII modification. The PII preparation used in this experiment was a mixture containing heterotrimers, formed by combining wild-type PII and PII containing the G89A subustitution in 1:10 ratio, and allowing random assortment of subunits. Steady state levels of PII modification were determined as in Materials and Methods, with the heterotrimeric PII present at 6 µM, 0.6 µM UTase/UR, 0.2 mM α-ketoglutarate, 0.5 mM UTP, 0.5 mM ATP, 1 mM DTT, and +/- 10 µM NRII. ●, - NRII; ■, + NRII.

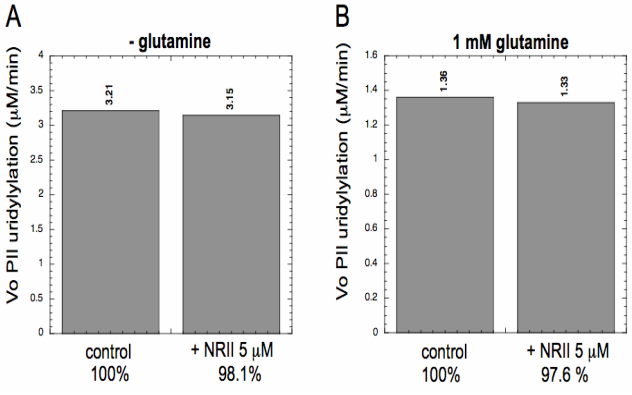

(4) Inhibition of the UT activity of the UTase/UR by NRII was lost when high concentrations of PII were used.

Figure S4. Lack of inhibition of the UT activity of when high concentrations of PII were used. The initial rate of PII uridylylation was measured as described previously (13) in the absence (**A**) or presence (**B**) of glutamine. For both panels, PII was present at 30 µM. For (**A**), UTase/UR was present at 0.05 µM; for (**B**) UTase/UR was present at

1 μM. Higher levels of enzyme were used for the experiment in panel B to allow the accurate measurement of rates in the presence of glutamine, where the UT activity was inhibited.

(5) Residual UT activity in the presence of glutamine.

Both the UT and UR activities demonstrated basal activities. The existence of a large basal activity for the UR reaction was well known (13), but the extent of a basal UT activity is reported here for the first time. It was observed that a basal UT activity of ~ 1 % of the maximal activity could not be ascribed to experimental noise and was probably due to incomplete enzyme regulation (Fig S5).

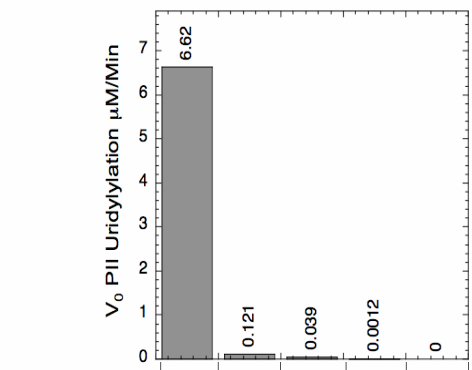

Glutamine (mM)	0	2.5	20	50	0
UTase/UR 0.04 μM	+	+	+	+	-
percent of control	100	1.83	0.59	0.018	0

Figure S5. Basal UT activity in the presence of glutamine. The initial rate of PII uridylylation was measured as described previously (13), with PII at 10 μM and UTase/UR at 0.04 μM, and with glutamine as indicated.

(6) Biphasic effects of NRII on PII uridylylation were still observed at 2 μM NRII.

Since modeling predicted that we should have been able to see biphasic effects of NRII at lower concentration that was used in most of our experiments (10 μM NRII), we examined effects of 2 μM NRII at three different glutamine concentrations. The glutamine concentrations were chosen such that NRII was expected to reduce PII uridylylation (0.1 mM glutamine), have no effect on PII uridylylation (0.29 mM glutamine), and increase PII uridylylation (2 mM glutamine), respectively.

Table S1. Comparison of effects of NRII at 2 μM and 5 μM at 3 glutamine concentrations.

	PII-UMP[1] μM (n)[2]		
[glutamine] mM	- NRII	2 μM NRII	5 μM NRII
0.1	6.36 (2.12)	5.76 (1.92)	5.58 (1.86)
0.29	5.78 (1.93)	4.89 (1.63)	5.03 (1.68)
2.00	1.27 (0.42)	2.08 (0.69)	3.48 (1.16)

[1]Reaction conditions were the same as for the experiments in Fig 2, except that the NRII concentration was as indicated. [100 mM Tris-Cl, pH 7.5, 25 mM $MgCl_2$, 100 mM KCl, 1 mM DTT, 3 μM PII, 0.8 μM UTase/UR, 0.2 mM α-ketoglutarate, 0.5 mM α-[^{32}P]-UTP, 0.5 mM ATP.]

[2]n cooresponds to the average number of modified subunits per PII trimer.

B. Calculation of n_H and S_{50}

The data is well described by a four-parameter Hill equation if the pairs (S_i,y_i) satisfy the relationship (ref S6)

$$y = (y_{\max} - y_{\min})\frac{S_{50}^{\ nH}}{S_{50}^{\ nH} + S^{nH}} + y_{\min}$$

where S is the stimulus, y is the response, y_{min} and y_{max} are the minimum and maximum level reached by the response and corresponding to zero or infinite stimulation respectively, S_{50} is the stimulus required to provide half-maximal response, and n_H is the Hill coefficient.

We fit the data to the equation above using the Ezyfit toolbox for Matlab obtaining good regression values (as indicated in Table S2). The four data sets and their corresponding fitting curves are plotted in Fig. S6.

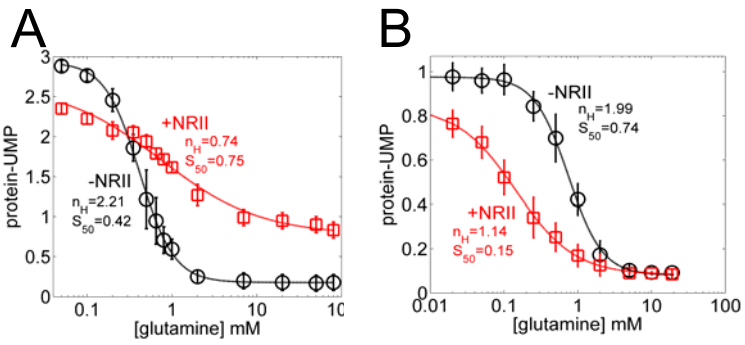

Figure S6. The data is well described by a four-parameter Hill equation. The experimental data for wild-type (**A**) and monovalent (**B**) PII is plotted superimposed with a four-parameter Hill curve. Note that in Figs. 2B and D in the main text the lines superimposed over the data are, instead, the best-fit output of the detailed kinetic model.

Error bars in the values of the fitted parameters (S_{50} and n_H) were obtained by fitting three different pairs of data: (S_i,y_i), $(S_i,y_i + \Delta y_i)$, and $(S_i,y_i - \Delta y_i)$, Δy_i being the error bar associated with y_i and obtained experimentally.

Table S2

Values of n_H and S_{50} for wild-type and monovalent PII

	Experiment	n_H	S_{50}	R
wild-type	-NRII	2.21±0.07	0.42±0.05	0.999
	+NRII	0.74±0.01	0.75±0.01	0.993
mutant	-NRII	1.99±0.18	0.74±0.15	0.999
	+NRII	1.14±0.05	0.15±0.04	0.999

Based on the intervals in Table S2 we can conclude that for wild-type PII the presence of NRII produces a statistically significant decrease in n_H and increase in S_{50} with p-values of 3e-6 and 3e-4, respectively. For monovalent PII, the presence of NRII produces a statistically significant decrease in both n_H and S_{50} with p-values of 0.001 and 0.002, respectively.

Fig. S7 compares the normalized responses of the systems containing wild-type and monovalent PII in the absence of NRII. The data was normalized between 0 and 1 following

$$y_{norm} = \frac{y - y_{\min}}{y_{\max} - y_{\min}}$$

The glutamine sensitivity of the two systems was quite similar as indicated in Table S2, there is not a statistically significant difference between both n_H values (p-values of 0.1). Thus, the trimeric structure of PII did not play a significant role in the glutamine sensitivity of the UTase/UR-PII cycle.

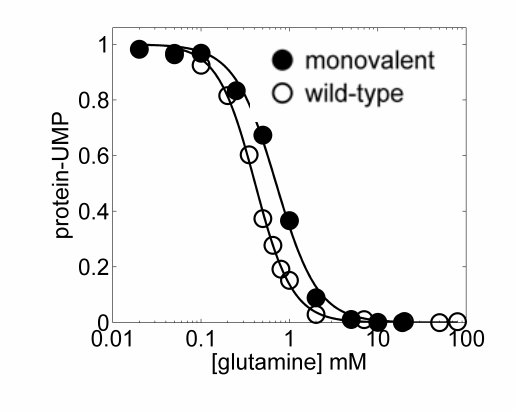

Figure S7. Comparison of the–NRII responses for wild-type and monovalent PII.

C. Predictions of a simple model allowing analytical solutions

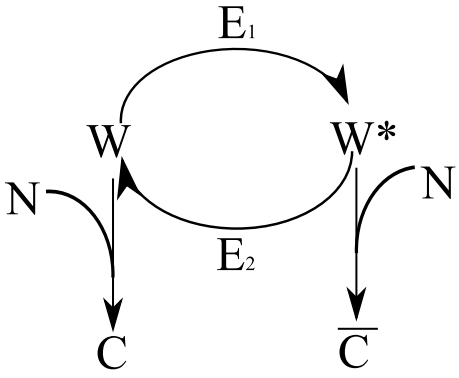

Figure S 8: Covalent modiþcation cycle subject to double loading.

We consider the covalent modiþcation cycle subject to loading on both active and inactive species as shown in Fig S8. Here, by loading we mean that the cycle is connected to a downstream component. We consider the standard two-step reaction model for enzymatic reactions. Let E_1 and E_2 be the converter enzymes that convert protein W to its active form W* and protein W* back to the inactive form W, respectively. Let C_1 denote the complex of E_1 with W and C_2 be the complex of E_2 with W*. The reactions for the system are given by

$$W + E_1 \underset{d_1}{\overset{a_1}{\rightleftharpoons}} C_1 \xrightarrow{k_1} W^* + E_1$$

$$W^* + E_2 \underset{d_2}{\overset{a_2}{\rightleftharpoons}} C_2 \xrightarrow{k_2} W + E_2,$$

to which we add the binding reaction of W with its downstream targets N in total amount N_T

$$W + N \underset{k_{off}}{\overset{k_{on}}{\rightleftharpoons}} C,$$

and the binding of W* also with downstream targets N

$$W^* + N \underset{\bar{k}_{off}}{\overset{\bar{k}_{on}}{\rightleftharpoons}} \not{C}.$$

The kinetic equations governing the system are given by

$$\begin{aligned}
\frac{dW}{dt} &= -a_1 W E_1 + d_1 C_1 + k_2 C_2 - k_{on} N W + k_{off} C \\
\frac{dC_1}{dt} &= a_1 W E_1 - (d_1 + k_1) C_1 \\
\frac{dW^*}{dt} &= -a_2 W^* E_2 + d_2 C_2 + k_1 C_1 - \not{k}_{on} N W^* + \not{k}_{off} \not{C} \\
\frac{dC_2}{dt} &= a_2 W^* E_2 - (d_2 + k_2) C_2 \\
\frac{dC}{dt} &= k_{on} N W - k_{off} C \\
\frac{d\not{C}}{dt} &= \not{k}_{on} N W^* - \not{k}_{off} \not{C}.
\end{aligned}$$

To this diPerential equations, we add the algebraic equations expressing the conservation laws for the protein and the enzymes:

$$W_T = W + W^* + C_1 + C_2 + C + \not{C},\ E_{1T} = E_1 + C_1,\ E_{2T} = E_2 + C_2,\ N_T = N + C + \not{C}.$$

Letting $K_D := k_{off}/k_{on}$ and $\not{K}_D := \not{k}_{off}/\not{k}_{on}$ and assuming that $K_D \gg W$ and that $\not{K}_D \gg W^*$, the steady state value of C and $\not{C}$ satisfy

$$C = \lambda W \text{ and } \not{C} = \alpha W^*, \text{ with } \lambda = \frac{N_T}{K_D} \text{ and } \alpha = \frac{N_T}{\not{K}_D}.$$

Note that in the case in which $\alpha = 0$, we have that $\not{C} = 0$ and we obtain as a special case of our derivations the situation in which the load is applied only on W.

From the conservation law for W in which we have neglected the complexes C_1 and C_2, we obtain that

$$W_T = W(1 + \lambda) + W^*(1 + \alpha). \tag{1}$$

Further, from setting $\frac{dC_1}{dt} = 0$ and $\frac{dC_2}{dt} = 0$, we obtain

$$C_1 = \frac{E_{1T} w}{K_1 + w} \text{ and } C_2 = \frac{E_{2T} w^*}{K_2 + w^*},$$

in which

$$w^* := \frac{W^*}{W_T},\ w := \frac{W}{W_T},\ K_1 := \frac{d_1 + k_1}{a_1 W_T},\ K_2 := \frac{d_2 + k_2}{d_2 W_T}.$$

From the equilibrium equation $k_1 C_1 = k_2 C_2$ and the conservation law $1 = w(1 + \lambda) + w^*(1 + \alpha)$ with

$$S := \frac{E_{2T} k_2}{E_{1T} k_1} \text{ and } \not{u}^* = w^*(1 + \alpha)$$

we obtain that ν^* (the response) satisfies the following equation that relates it with the stimulus (S)

$$S = \frac{(1-\nu^*)(K_2(1+\alpha)+\nu^*)}{\nu^*(K_1(1+\lambda)+1-\nu^*)}. \tag{2}$$

Effect of N_T on the value of Hill coefficient and S_{50}

In order to calculate the effect of the load N_T on the Hill coefficient n_H, we use the response coefficient R. Since ν^* is a decreasing function of S, the response coefficient is defined as the ratio between the value of S corresponding to 10% of the maximal value of ν^* and the value of S corresponding to 0% of the maximal value of ν^*:

$$R := \frac{S_{10}}{S_{90}}.$$

For a Hill equation, this coefficient satisfies

$$R = (81)^{1/n_H},$$

that is, R decreases with n_H. Therefore, we can take R as a measure of the Hill coefficient resulting from equation (2).

The maximal value of ν^* corresponds to when $w = 0$ and is obtained from $1 = w(1+\lambda) + w^*(1+\alpha)$ as

$$\nu_{max} = 1.$$

As a consequence, we have that

$$R = \frac{S_{10}}{S_{90}} = 81\frac{(K_1(1+\lambda)+0.1)}{(K_1(1+\lambda)+0.\ )}\frac{(K_2(1+\alpha)+0.1)}{(K_2(1+\alpha)+0.\ )},$$

which is a monotonically increasing function of N_T. For the case of no load, i.e., $\alpha = \lambda = 0$, R reduces to the same expression obtained by Goldbeter and Koshland (14), while when the load tends to infinity we have that $R = 81$, corresponding to Hill coefficient $n_H = 1$. In the case in which the load is applied only on W, that is, $\alpha = 0$, we obtain the same behavior for R and thus for the Hill coefficient n_H. However, while with load applied on both W and W^* we have that R tends to 81 for large N_T *independently* of the parameters K_1 and K_2, when the load is applied to W only, we have that $R = 81\frac{K_2+0.1}{K_2+0.9}$ for $N_T \to \infty$, which depends on K_2 and tends to 81 only when K_2 is sufficiently large.

The expression of S_{50} is given by

$$S_{50} = \frac{(K_2(1+\alpha)+0.5)}{(K_1(1+\lambda)+0.5)}.$$

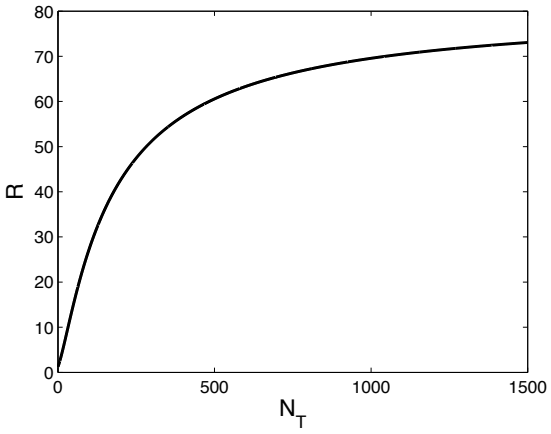

Figure S : Effect of the load N_T on the value of R. Here, $K_1 = K_2 = 0.01$.

Computing the derivative of S_{50} with respect to N_T, we obtain that the S_{50} increases with N_T if

$$\frac{K_2}{K_d}(K_1 + 0.5) > \frac{K_1}{K_d}(K_2 + 0.5),$$

otherwise it decreases with N_T. In the case in which $\frac{K_2}{K_d}(K_1 + 0.5) = \frac{K_1}{K_d}(K_2 + 0.5)$, the value of S_{50} does not change with N_T. In the case in which the load is applied only on W, that is, $\alpha = 0$, we obtain that S_{50} is a monotonically decreasing function of the load N_T.

Effect of N_T on the steady state value of w^*

In order to study the behavior of the steady state value of w^* when N_T is varied, we solve equation (2) for w^*. This gives a second order equation in w^*, whose root between 0 and 1 is given by

$$w^* = \frac{(1 - K_2 - S(K_1 + 1)) + \sqrt{(1 - K_2 - S(K_1 + 1))^2 + 4(1 - S)K_2}}{2(1 - S)}, \qquad (3)$$

in which we have denoted $K_2 := K_2(1 + N_T/K_d)$ and $K_1 := K_1(1 + N_T/K_d)$. We study the derivative with respect to N_T of this steady state expression for two limit cases: $S \ll 1$ and $S \gg 1$.

Case 1: $S \ll 1$. By computing the derivative with respect to N_T and using that $S \ll 1$, we obtain that $\frac{d\bar{w}^*}{dN_T} < 0$ if

$$(K_2/K_d)^2 < K_2(1 + N_T/K_d) + S(K_1K_2)/(K_dK_d)(1 - K_2 - SK_1),$$

which for $S \ll 1$ can be satisfied if $K_2 < K_d(N_T + K_d)$.

Case 2: $S \gg 1$. In this case, the steady state expression of $\bar{u}^*$ is well approximated by

$$\bar{u}^* \approx \frac{S(\bar{K}_1 + 1) - \sqrt{S^2(\bar{K}_1 + 1)^2 - 4S\bar{K}_2}}{S},$$

whose derivative with respect to N_T is positive if

$$S(K_1K_2)/(K_d\bar{K}_d)(\bar{K}_1 + 1) > (K_2/\bar{K}_d)^2 + S\bar{K}_2(K_1/K_d)^2,$$

which for $S \gg 1$ is satisfied if $K_1 + 1 > K_1(\bar{K}_d/K_d)$, which in turn is satisfied if $\bar{K}_d \leq K_d$.

In the case in which the load is applied only on W, that is $\alpha = 0$, the steady state expression (3) reduces to

$$\bar{u}^* = \frac{(1 - K_2 - S(K_1(1 + \lambda) + 1)) + \sqrt{(1 - K_2 - S(K_1(1 + \lambda) + 1))^2 + 4(1 - S)K_2}}{2(1 - S)}.$$

Letting $B(\lambda) := 1 - K_2 - S(K_1(1 + \lambda) + 1)$, we consider two cases: $B(\lambda) > 0$ and $B(\lambda) < 0$. When $B(\lambda) > 0$, B is a decreasing function of λ so that also $\bar{u}^*$ is a decreasing function of λ and thus of N_T. When $B(\lambda) < 0$, we can re-write $\bar{u}^*$ as $\bar{u}^* = 2K_2/(|B| + \sqrt{B^2 + 4(1 - S)K_2})$ in which $|B|$ is an increasing function of λ so that $\bar{u}^*$ is a decreasing function of λ and thus of N_T. Therefore, for every value of S, when the load is applied to W only, the steady state $\bar{u}^*$ always decreases with the load N_T. This is depicted in Fig S10. The effect of the load N_T on the value of R is summarized in Fig S . As predicted from theory, the maximal value reached by R for very high load N_T never exceeds 81. The effects of the load N_T on the shape of the steady state response and on the S_{50} for different values of the dissociation constants K_d and $\bar{K}_d$ are summarized in Fig S11.

Lower limit of Hill coefficient n_H for large loads

Our calculations predict that for $N_T \to \infty$, the value of R approaches 81 and thus the Hill coefficient n_H approaches 1. This is also a lower limit for n_H as R is a monotonically increasing function of N_T. The experimental results with the trimer, however, indicated a value lower than 1 for the Hill coefficient when large amounts of load N_T were applied. In order to investigate what mechanism could give rise to subsensitivity ($n_H < 1$), we added to the simple model of Fig S8 the possibility of the conversion between the complexes C and $\bar{C}$ due to covalent modification. We

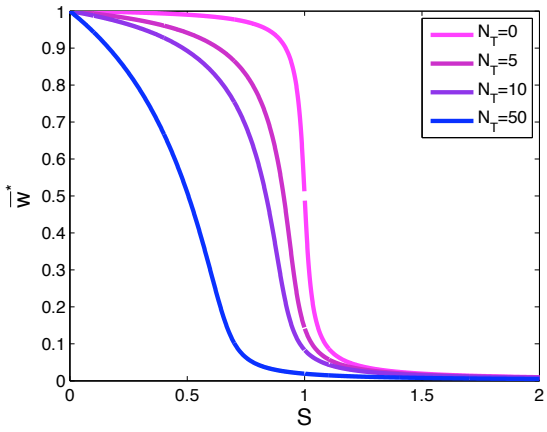

Figure S 10: Effect of the load on the steady state response of $\bar{w}^*$ to S when the load is applied only to W, that is, $\alpha = 0$. increasing the load decreases the steady state for all values of S.

thus explored the possibility of obtaining an upper limit for R higher than 81 (a lower limit for n_H lower than 1) by adding the two conversion reactions

$$\mathrm{C} \xrightarrow{k_f} \mathrm{C}' \text{ and } \mathrm{C}' \xrightarrow{k_r} \mathrm{C}.$$

Adding these reactions, we obtain the new steady state values for the complexes C and C' as

$$C' = \frac{N_T\left(W^* + \frac{\bar{a}}{K_d+a}W\right)}{K_d + b\frac{K_d}{K_d+a}},\ C = \frac{N_T\left(W + \frac{b}{\bar{K}_d+b}W^*\right)}{K_d + a\frac{\bar{K}_d}{\bar{K}_d+b}},$$

in which $a = k_f/k_{on}$, $\bar{a} = k_f/\bar{k}_{on}$, $b = k_r/k_{on}$ and $\bar{b} = k_r/\bar{k}_{on}$. By employing $W_T = W + W^* + C + C'$, $\bar{W}^* = W^* + C'$, and solving $k_1 C_1 = k_2 C_2$ for S, we obtain

$$S = \frac{w(K_2 + w^*)}{w^*(K_1 + w)},$$

in which

$$w^* = \frac{\bar{w}^* - N_T(D/A)}{G - N_T(B\ D/A)},\ w = \frac{1 - Bw^*}{A},$$

where

$$A = 1 + \frac{N_T}{K_d + \frac{a\bar{K}_d}{\bar{K}_d+b}} + \frac{N_T\frac{\bar{a}}{K_d+a}}{K_d + \frac{\bar{b}K_d}{K_d+a}},\ B = 1 + \frac{N_T}{K_d + \frac{\bar{b}K_d}{K_d+a}} + \frac{N_T\frac{b}{\bar{K}_d+b}}{K_d + \frac{a\bar{K}_d}{\bar{K}_d+b}},$$

$$G = 1 + \frac{N_T}{K_d + \frac{\bar{b}K_d}{K_d+a}},\ D = \frac{\frac{\bar{a}}{K_d+a}}{K_d + \frac{\bar{b}K_d}{K_d+a}}.$$

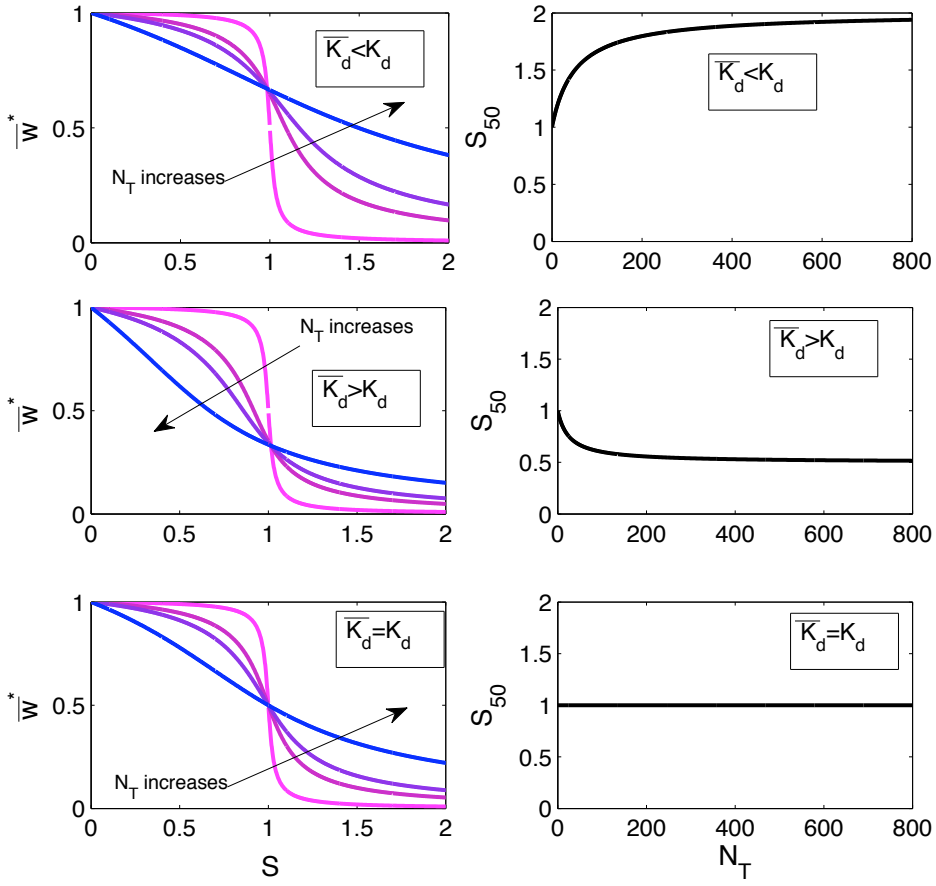

Figure S 11: Effect of the load N_T on the shape of the steady state response of $\bar{w}^*$ and on the S_{50} for different values of the ration of $K_d/\bar{K}_d$. In all plots, $K_1 = K_2 = 0.01$ In the top plots, $K_d/\bar{K}_d > 1$ resulting in the S_{50} being an increasing function of the load N_T and in the crossing point of the steady state curves for different values of N_T being above 0.5. In the middle plots, $K_d/\bar{K}_d < 1$ resulting in the S_{50} being a decreasing function of the load N_T and in the crossing point of the steady state curves for different values of N_T being below 0.5. In the bottom plots, $K_d/\bar{K}_d = 1$ so that the value of S_{50} does not change with the load N_T and all steady state curves cross at 0.5.

The resulting plot for R as a function of N_T is reported in Fig 12. As the rates of modiþcation between the two complexes are increased, the value of R approaches values larger than 81 for large loads N_T. This corresponds to reaching values of the Hill coeŽcient n_H smaller than 1, thus attaining subsensitivity.

If we let $k_f = k_1' E_1$ and $k_r = k_2' E_2$ so that $a = k_1' E_1 / k_{on}$, $b = k_1' E_1 / k_{on}$,

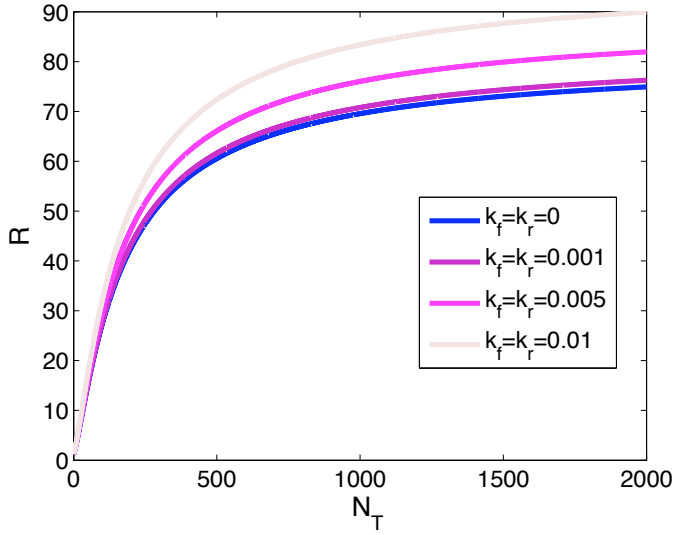

Figure S 12: Effect of adding a reversible covalent modification between the complexes C and $\bar{\text{C}}$. In this plot, we have taken $K_1 = K_2 = 0.01$, $K_d = \bar{K}_d = 1$, $k_{on} = \bar{k}_{on} = 1$. As the rates of modification between the complexes increase, the value of R approaches values larger than 81 for large N_T.

$b = k_2' E_2/k_{on}$ and $\bar{b} = k_2' E_2/\bar{k}_{on}$, with $E_1 = K_1 E_{1T}/(K_1 + w)$ and $E_2 = K_2 E_{2T}/(K_2 + w^*)$, the above expressions become substantially more complex. However, under the simplifying assumptions that

$$K_d \gg \frac{k_1' E_1}{k_{on}}, \text{ and } \bar{K}_d \gg \frac{k_2' E_2}{\bar{k}_{on}},$$

we have that

$$\bar{C} = \frac{N_T\left(W^* + \frac{\bar{a}}{K_d} W\right)}{\bar{K}_d}, \; C = \frac{N_T\left(W + \frac{b}{K_d} W^*\right)}{K_d}.$$

Employing the conservation law $1 = w + w^* + C/W_T + \bar{C}/W_T$, the substitution $\bar{w}^* = w^* + \bar{C}/W_T$, solving $k_1 C_1 = k_2 C_2$ for E_{2T}, and considering that in the limit of large loads N_T we have $w^* \ll K_1$ and $w \ll K_2$, we finally obtain that

$$\frac{E_{2T}}{E_{1T}} \approx \frac{\alpha(1 - \bar{w}^*)}{\bar{w}^*\left(\lambda(1 + \bar{V}_1/K_1) + \alpha E_{1T} k_2'/(K_d k_{on})\right) - \alpha \bar{V}_1/K_1},$$

in which $\bar{V}_1 = k_1' E_{1T}/(\bar{k}_{on} \bar{K}_d)$. Assuming that $k_1', k_2' \ll 1$, we have that the maximal and minimal values of $\bar{w}^*$ are approximatively 1 and 0, respectively. Letting $y := \frac{E_{2T}}{E_{1T}}$ and denoting by y_{10} the value of y corresponding to $\bar{w}^* = 0.1$ and

by y_{90} the value of y corresponding to $W^* = 0.$, we obtain that

$$\lim_{N_T \to \infty} \frac{y_{10}}{y_{90}} = 81 \frac{\frac{1}{K_d}\left(1 + \frac{\bar{V}_1}{K_1}(1 - 1.1(K_d/K'_d))\right) + E_{1T}k'_2/(K'_d K_d k_{on})}{\frac{1}{K_d}\left(1 + \frac{\bar{V}_1}{K_1}(1 - 10(K_d/K'_d))\right) + E_{1T}k'_2/(K'_d K_d k_{on})},$$

in which the numerator is larger than the denominator and as a consequence this limit is equal to a number greater than 81. As a consequence, the Hill coefficient n_H for very large values of N_T can reach values smaller than 1.

Conclusions from the model

From this study, we conclude the following on the effect of the load on the steady state response of $W^* + C'$ for the covalent modification cycle of Fig S8:

Effect on the steady state value. When there is load applied to W only, increasing the load decreases the steady state value for all input stimuli $S = V_2/V_1$. By contrast, when loading is applied to both W and W*, an increased load decreases the steady state value for low S, while it increases it for high values of S.

Effect on S_{50}. When there is load applied to W only, increasing the load decreases the value of S_{50}. By contrast, when the load is applied to both W and W*, increasing the load can either monotonically increase the value of S_{50} or monotonically decrease it. Furthermore, it is possible to establish the ratio between the dissociation constants K_d and K'_d so that increasing the load has no effect on the value of S_{50}.

Effect on n_H. The value of n_H always monotonically decreases with the load. In particular, if the load is applied to W only, the value of n_H for large loads depends on the value of K_2 and tends to 1 if K_2 is large enough. By contrast, when the load is applied to both W and W*, for large loads the value of n_H approaches 1 *independently* of the values of the parameters. Furthermore, if a reversible modification occurs between the complexes C and C', then n_H can achieve values smaller than 1 for large enough loads (subsensitivity).

D. A detailed kinetic model for the UTase/UR-PII cycle and the effects of NRII

(1) Model description

1.1 Regulation of UTase/UR enzyme by glutamine

Glutamine controls the UTase/UR enzyme: for low glutamine concentrations there are high UT and low UR activities, while for high glutamine concentrations the situation is the opposite. We have considered that from the total UTase concentration, there is a small fraction that remains inactive, meaning that it does not have UT or UR activity and does not bind glutamine. The model also considers that there are small fractions of the total UTase/UR enzyme concentration that have basal UT activity (meaning that has UT activity even when there is very high glutamine concentration) and basal UR activity (has UR activity even when there is no glutamine). This situation was addressed experimentally as indicated in FigS5. The remaining enzyme is susceptible to be converted from the UT state into the UR state by the action of glutamine. These considerations are mathematically articulated as follows:

$$UTase = UTase_{inactive} + UT_{basal} + UR_{basal} + UT + UR$$

$$UTase = \alpha UTase + \beta UTase + \gamma UTase + \delta UTase \quad \text{with} \quad \alpha + \beta + \gamma + d = 1 \quad \text{and} \quad \alpha, \beta, \gamma, \delta \leq 1$$

$$UT + gln \underset{f'}{\overset{f}{\rightleftarrows}} UR \quad \text{with} \quad UR = \delta UTase - UT$$

$$UT = \frac{\delta UTase}{1 + gln / K_d} \quad \text{with} \quad K_d = f'/f$$

The last equation provides the steady-state concentration of the enzyme in its UT form for a given glutamine concentration.

1.2 Uridylylation/Deuridylylation reactions

Variable P_{ijk} indicates the modification (uridylylation) state of the trimeric protein PII. Subindexes i, j, k represent the state of each of the three subunits forming the protein PII, they can take the values 0 or 1, meaning that the corresponding subunit is not/is uridylylated.

Since the three subunits are considered to be identical, we thus denote P_x with x=0, 1, 2, or 3, as the states of PII that have 0, 1, 2, or 3 modified subunits, respectively. For example, P_{100}, P_{010}, and P_{001} are all labeled as P_1, meaning that PII has a single uridylyl group. There are then three possible ways to go from P_0= P_{000} to P_1, i.e. binding the UTase enzyme in its UT form in any of the three subunits. On the other hand, given a state in the P_1 group, P_{100} for example, there

is only one way to go to P_0, which is by the binding of the UTase enzyme in its UR form in the uridylylated subunit, which is the first one in the case of P_{100}.

The following reactions represent the reversible transition that P_x can undergo (for the UT reaction x=0, 1, 2; for the UR reaction x=1, 2, 3).

$$P_x + UT \underset{d}{\overset{a}{\rightleftarrows}} C_x \xrightarrow{k_{cat}} P_{x+1} + UT$$

$$P_{x+1} + UR \underset{d'}{\overset{a'}{\rightleftarrows}} C_x' \xrightarrow{k'_{cat}} P_x + UR$$

We consider that the association (*a* and *a'*), dissociation (*d* and *d'*) and catalytic (k_{cat} and k_{cat}*'*) rates are identical no matter the actual value that x takes. C_x and C_x' represent the intermediate substrate-enzyme complexes in the enzymatic reactions.

1.3 PII-NRII binding

In each unmodified subunit, PII is able to bind the protein NRII, which is itself a dimer. Due to the size and conformation of protein NRII, it is unlikely to find more than one NRII protein bound to PII simultaneously, and this scenario has not been detected experimentally.. This possibility was therefore not included in the model.

Because of the binding with NRII, the index representing each subunit of protein PII could be 0, 1, or n (actually, n or ñ, representing each of NRII identical subunits), indicating that is neither modified or bound to NRII (0), modified (1), or bound to NRII (n). For example, P_{1n0} indicates a complex PII-NRII in which PII is only modified in the first subunit and the binding with NRII occurs in the second subunit. Since the subunits are identical, this state is completely equivalent to states P_{10n}, P_{n10}, P_{01n}, P_{n01}, P_{0n1}, and also to all of the states that result if in the previous ones n is replaced by ñ.

We then denote N_x with x=0, 1, or 2, all the complexes PII-NRII in which PII has 0, 1, or 2 modified subunits, respectively (it can not be a 3 because PII having 3 modified subunits is unable to bind NRII). In group N_0, for example, we have P_{n00}, P_{0n0}, P_{00n}, and also $P_{ñ00}$, $P_{0ñ0}$, $P_{00ñ}$.

The following reaction represents the reversible binding of NRII: $NRII + P_x \underset{b_x'}{\overset{b_x}{\rightleftarrows}} N_x$

We have considered that the binding rates, b_x and b_x*'* depend on the uridylylation state of the PII that is being bound, resulting in three pairs of binding and unbinding rates (b_o, b_o*'*), (b_1,

b_1'), and (b_2, b_2'). It is possible for a complex PII-NRII to also bind UTase in its UT or UR forms, leading to the following reactions:

$$N_x + UT \underset{\tilde{d}}{\overset{\tilde{a}}{\rightleftarrows}} \tilde{C}_x \xrightarrow{\tilde{k}_{cat}} N_{x+1} + UT$$

$$N_{x+1} + UR \underset{\tilde{d}'}{\overset{\tilde{a}'}{\rightleftarrows}} \tilde{C}_x' \xrightarrow{\tilde{k}'_{cat}} N_x + UR$$

We have assumed that the binding rates between the complex PII-NRII and enzymes UT or UR may differ from those of PII with UT or UR. We have label them as $\tilde{a}, \tilde{d}, \tilde{k}_{cat}, \tilde{a}', \tilde{d}', \tilde{k}'_{cat}$.

1.4 NRII binding simultaneously two PII proteins

NRII is able to bind two PII proteins simultaneously, one with each of its subunits. For example, state $PP_{n00\text{-}ñ00}$ indicates that one PII protein is bound in its subunit i to subunit n of the NRII protein, while another PII protein is bound also in its subunit i to subunit ñ of the same NRII protein. As before, since all the three PII subunits and the two NRII subunits are identical, there are several states that are equivalent. In this way, we use a simplified notation, N_{xy}, x and y could take the values 0, 1, 2 depending on how many uridylylated subunits each of the bound PII has. Also, $N_{xy} = N_{yx}$. In N_{00} group, for example, we have $PP_{n00\text{-}ñ00}$, $PP_{n00\text{-}0ñ0}$, $PP_{n00\text{-}00ñ}$, $PP_{0n0\text{-}ñ00}$, $PP_{0n0\text{-}0ñ0}$, $PP_{0n0\text{-}00ñ}$, $PP_{00n\text{-}ñ00}$, $PP_{00n\text{-}0ñ0}$, and $PP_{00n\text{-}00ñ}$.

The following reaction represents the reversible binding of the complex PII-NRII to another PII protein: $N_x + P_y \underset{\bar{b}_y'}{\overset{\bar{b}_y}{\rightleftarrows}} N_{xy}$

As before, we have considered that the binding rates, $\bar{b}_y$ and $\bar{b}_y'$ depend on the uridylylation state of the PII that is being bound, resulting in three pairs of binding and unbinding rates ($\bar{b}_0$, $\bar{b}_0'$),($\bar{b}_1$, $\bar{b}_1'$) , and ($\bar{b}_2$, $\bar{b}_2'$). We consider that a complex PII-NRII-PII can also bind UTase in its UT or UR forms. In this way, a configuration in group N_{00} for example, can lead to a new one in group N_{10} or in group N_{01} by binding UT. We have assumed that the binding rates between a complex PII-NRII-PII and enzymes UT and UR may differ from those of PII alone and those of PII-NRII. We label them as $\bar{a}, \bar{d}, \bar{k}_{cat}, \bar{a}', \bar{d}', \bar{k}'_{cat}$ respectively.

1.5 Monovalent and Divalent forms of PII

In order to model the different uridylylation and NRII-binding states of the monovalent and divalent PII proteins generated experimentally, we adapted our model for the homotrimeric PII. In the monovalent case, there is only one functional subunit that is either uridylylated, bound to NRII, or neither of them. There are fewer states to be considered then, as indicated in FigS13B. For the divalent case, there are two functional subunits, so an intermediate repertoire of states is allowed, as illustrated in FigS14 (see below).

1.6 Model equations and parameters optimization

We used a system of ordinary differential equations to describe the temporal evolution of the variables representing the proteins PII, NRII, the enzyme UTase/UR, and the complexes between them, in their different states: PII could have 0, 1, 2, or 3 of its subunits modified; NRII could be free, bound to 1 or 2 PII proteins, each one with different modification states; the enzyme UTase/UR could be in its UT or its UR conformation, free or bound to PII, a complex PII-NRII, or a complex PII-NRII-PII. The kinetic equations describing the temporal evolution of these variables come from the use of the law of mass action. The variables represent the concentration of a given species. Since the experiments are done in a test tube, the system is closed, meaning that proteins are not produced or degraded, leading to conserved quantities, such as the total amount of PII, NRII, and UTase/UR.

The quantity that is experimentally measured is the amount of protein bound to UMP, which is indicated as P_{UMP} and includes states P_1, P_2, and P_3 of protein PII; states N_1 and N_2 of the complex PII-NRII, since in them PII has 1 or 2 modified subunits; all the states N_{xy} representing the complex NRII-PII-NRII, except for N_{00} since here NRII is bound to two unmodified PIIs; and the corresponding intermediate complexes formed by the binding of P_x, N_x, or N_{xy} with UT or UR. The states contributing to P_{UMP} can do it with a factor 1 (like P_1, which has only one UMP group bound to PII), 2 (for example P_2, N_2 or N_{11}), 3 or 4.

The set of coupled ordinary differential equations was integrated in MATLAB 7.7.0 (Mathworks, Natick, MA) until reaching the steady state. The parameters involved were optimized so that the output of the model provides a good representation of the experimental data in Fig2B and Fig2D. The initial guesses for the parameters were taken from the literature whenever possible (13, ref S3). Given those initial guesses for the parameters and an interval of variation for each of them defined based on experimental considerations, a random exploration

was performed in order to minimize a cost function measuring the distance between the output of the model and the experimental data, weighted by the corresponding error bars. For the data related to trimeric PII (Fig 2B) a dual optimization was performed in order to minimize simultaneously the cost functions related to -NRII and +NRII curves. Once these optimizations were obtained, the same procedure was applied for the mutant data (Fig 2D). Only those parameters related to PII-UT and PII-UR interactions were slightly adjusted (allowing them to change only by <20% with respect of what was obtained for trimeric PII). Also, it is known that in the mutant scenario there are still some percentages of trivalent and divalent PII (12). This observation was taken into account and those percentages were optimized to better reproduce the experimental data.

Of course multiple sets of parameters fit the model equally well, a common problem in complex biochemical models (ref S7-S9). For example, when we removed the constraint of UR basal activity being between 20% and 30% of the maximal activity, we obtained a different set of parameters from fitting of the data to the model. The model contains 49 variables and 37 parameters. Thirteen of the parameters have been determined experimentally, 24 of the parameters have been determined only with the model; among these several were constrained based upon assumed ratios of parameters. Our data set consists of 46 data points with error bars (mainly from two determinations). If exact measurements were possible, a minimum of 75 data points would be required for the determination of 37 parameters, or a minimum of 49 data points would be required for determination of 24 parameters (ref S9). Based on this number of data points and variables, the parameters are somewhat under-determined (ref S7-S9). Simulations using the parameters in Table S3 and Table S4 showed kinetics of reaching the steady-state similar to that observed in the experiments. Thus the parameterized model seems to mimic the experimental system reasonably well.

(2) Schemes representing the model

The upper level in both panels of FigS13 describes PII modification state; the subindex in P indicating how many subunits are modified (ranging from 0 to 3 in the case of wild-type PII). A single PII trimer binding more than one NRII dimer simultaneously has not been experimentally observed, and therefore that scenario was not included in the model. Perhaps the binding of NRII to one of the subunits of the PII trimer blocks the binding of additional NRII

dimers to the other subunits of the PII trimer.

During the course of another research project by our group we observed that under the conditions of our experiments, NRII dimers each bound to two PII trimers, and did so with significant cooperativity (ref. S3). Thus, our scheme for the system containing wild-type PII includes complexes in which a single NRII dimer is bound bind to two PII proteins, with each NRII subunit binding a PII trimer (FigS13). Since we demonstrated that NRII binds to partially modified PII trimers (by their unmodified subunit), such complexes were also included in the model (FigS13). For complexes containing NRII and PII, N_i designates an NRII-PII complex where PII has *i* modified subunits, while N_{ij} indicates a PII-NRII-PII complex, where one PII has *i* modified subunits and the other one has *j* modified subunits (FigS13). Thus, transitions between states involving PII and NRII binding and unbinding, as well as changes in PII modification catalyzed by the UTase/UR are depicted in FigS13.

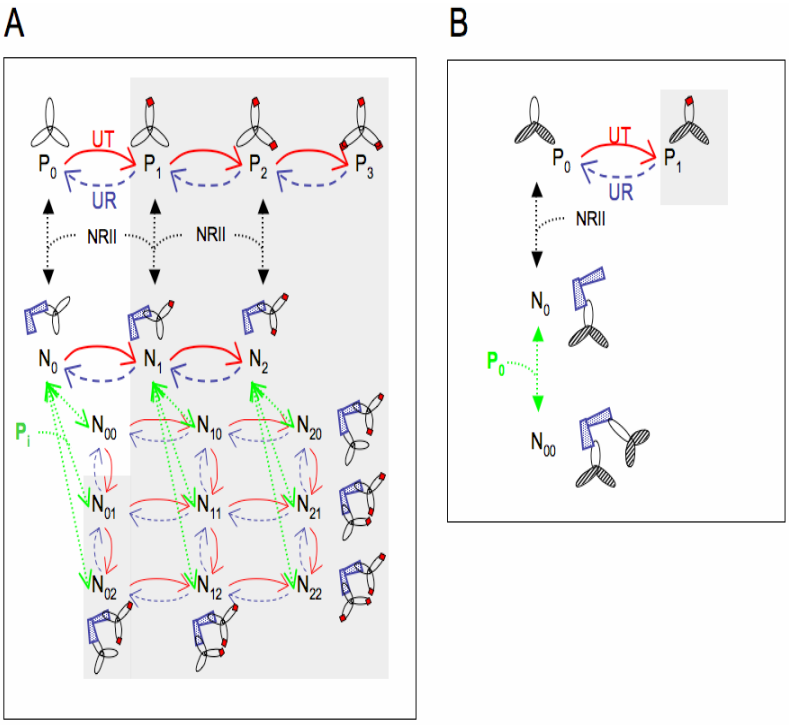

Figure S13. A detailed kinetic model for the UTase/UR-PII cycle and the effects of NRII. Schemes representing the models for **(A)** wild-type and **(B)** monovalent PII, respectively. The UT activity of the UTase/UR enzyme is indicated with solid red arrows, while its UR activity is indicated with dashed blue arrows. UMP groups are represented by a red square over the PII subunits. Shadowed areas over each scheme indicate the variable that is measured, denoted as protein-UMP.

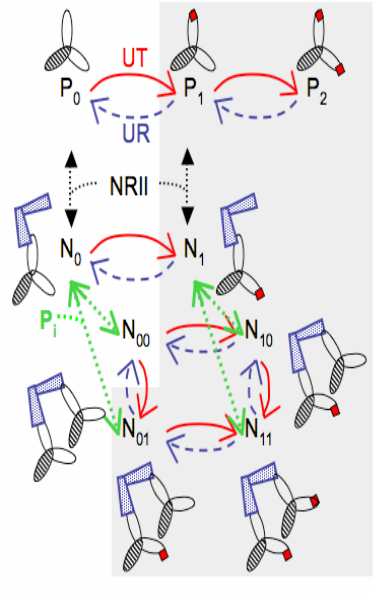

Figure S14. Scheme representing the model for "divalent" PII. As in FigS13, the UT activity of the UTase/UR enzyme is indicated with solid arrows, while its UR activity is indicated with dashed arrows. UMP groups are represented by a red squares over the PII subunits. The shadowed area over the scheme indicates the variable that is measured, denoted as protein-UMP. The inactive subunits of the divalent PII are indicated with stippling.

(3) The parameters in the model

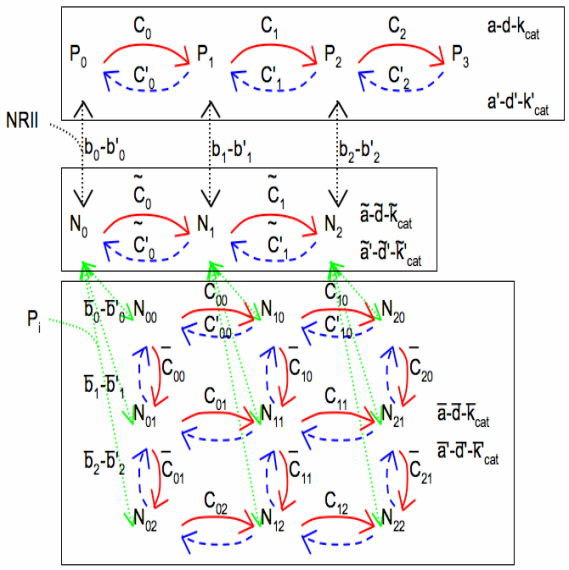

Figure S15. The parameters in the detailed kinetic model for the UTase/UR-PII cycle and the effects of NRII. Model parameters are indicated over the scheme. C and C' represent the substrate-enzyme complexes for the UT and UR reactions, respectively. Sub-and super-indexes on C and C' stand for the different complexes, depending on the degree of modification PII has, and whether it is bound to NRII or not. Rates *a*, *d*, and *kcat* are the association, dissociation, and catalytic constants for the enzymatic reactions. Rates *b* and *b'* are the association and dissociation rates between PII and NRII.

Table S3. A. Parameters from fitting data to the model.

Parameter	**Literature**[1]	**Model**
Gln-UTase/UR		
Kd	0.08 mM	0.06 mM
inactive UTase		0.8%

basal UT		1.7%
basal UR	20-30 %	21.8%
PII-UT		
kcat	137/min	34.4/min
Km	3.0 μM	1.3 μM
Kd	1.8 μM	1.1 μM
PII-UR		
kcat	2.7/min (- gln) 6.5/min (2.5 mM gln)	5.2/min
Km	2.3 μM (- gln) 1.2 μM (1 mM gln) 0.82 μM (2.5 mM gln)	1.7 μM
Kd	2.0 μM	1.4 μM
PII-NRII		
Kd P_0-NRII	0.3 μM	1.2 μM
Kd P_1-NRII		5.9 μM
Kd P_2-NRII		5.7 μM
(PII-NRII)-PII		
Kd (Pi-NRII)-P_0		0.2 μM
Kd (Pi-NRII)-P_1		1.2 μM
Kd (Pi-NRII)-P_2		0.1 μM

Table S3. B. Comparison of different complexes.

Parameter	**PII-UT**	**(PII-NRII)-UT**	**(PII-NRII-PII)-UT**
kcat	34.4/min	192.0/min	6.8/min
Km	1.3 μM	3.1 μM	4.8 μM
Kd	1.1 μM	0.8 μM	4.5 μM
Parameter	**(PII-UMP)-UR**	**[(NRII-(PII-UMP)]-UR**	**[(PII-NRII-(PII-UMP)]-UR**
kcat	5.2/min	3.9/min	2.9/min
Km	1.7 μM	4.5 μM	17.8 μM

Kd	1.4 μM	4.0 μM	16.2 μM

---

[1]Values for parameters were obtained from (13) and (ref S3).

Table S4. A. Comparison of Parameters for wild-type PII and heterotrimer PII

Parameter	wild-type PII	heterotrimer PII
PII-UT		
kcat	34.4/min	40.5/min
Km	1.3 μM	1.2 μM
Kd	1.1 μM	0.98 μM
PII-UR		
kcat	5.2/min	4.2/min
Km	1.7 μM	2.24 μM
Kd	1.4 μM	2.0 μM

Table S4. B. Comparison of expected distirbution of subunits into heterotrimers if random assortment vs distribution of subunits determined from fitting of the model.

Species	Expected if random assortment	Fitting of Model to Data
monovalent PII	85 %	80 %
divalent PII	14 %	16 %
trivalent (wild-type) PII	1 %	4 %

(4) Predictions of the model

An alternative way to consider the data in Fig 5A and Fig 5B is by the reverse stimulus-response plot, where the response of the system is considered as a function of the downstream component. This plot highlights retroactive effects. NRII decreased uridylylation at low glutamine concentrations and increased urilylylation at high glutamine concentrations (Fig S16A). The net effect of NRII was thus to maintain the modification state of PII at an intermediate level. In simulations of the system utilizing monovalent PII, both NRII and

glutamine reduced the extent of PII modification. The reverse stimulus-response plot highlights the monotonic nature of NRII effects in this system

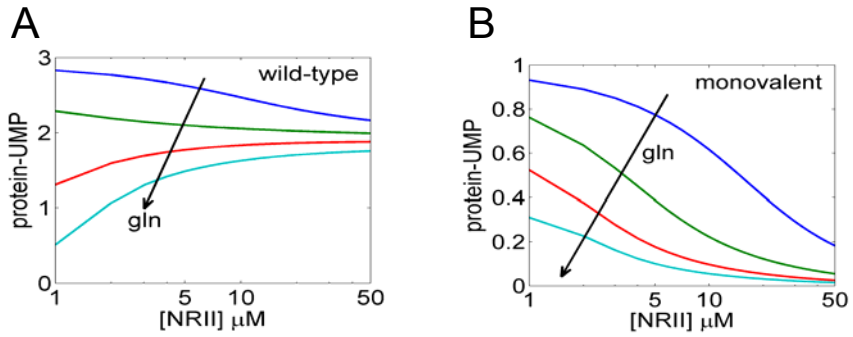

Figure S16. Reverse-stimulus response curves. Stimulus response curves obtained with the kinetic model for wild-type PII **(A)** or monovalent PII **(B)**, using NRII as the stimulation for different levels of glutamine (0.05, 0.2, 0.5 and 1 mM).

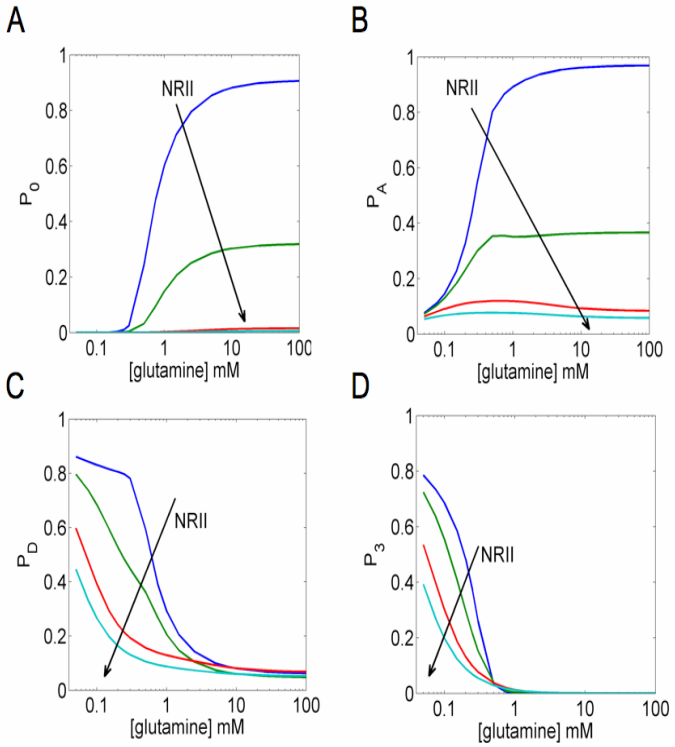

Figure S17. Predictions of the detailed kinetic model on the effect of NRII on the steady-state level of different modified forms of PII. Stimulus response curves obtained with the kinetic model for wild-type PII, using glutamine as the stimulation and measuring the response in (**A**) P_0, (**B**) $P_A = P_0 + P_1 + P_2$, (**C**) $P_D = P_1 + P_2 + P_3$, (**D**) P_3 for different concentrations of NRII (0, 1, 5, and 10 μM).

(5) Model equations

The original Matlab files of the model are available from aninfa@umich.edu.

$$
\begin{aligned}
&dP_1/dt = k_{cat}C_0 - (a'P_1UR - d'C_0') - 2(aP_1UT - dC_1) + 2k_{cat}'C_1' - 4(b_1P_1N - b_1'N_1) - \\
&\quad - 6(\bar{b}_1N_0P_1 - \bar{b}_1'N_{01}) - 12(\bar{b}_1N_1P_1 - \bar{b}_1'N_{11}) - 6(\bar{b}_1N_2P_1 - \bar{b}_1'N_{21}) \\
&dC_0/dt = aP_0UT - (d + k_{cat})C_0 \\
&dC_0'/dt = a'P_1UR - (d' + k_{cat}')C_0' \\
\\
&dP_2/dt = 2k_{cat}C_1 - 2(a'P_2UR - d'C_1') - (aP_2UT - dC_2) + k_{cat}'C_2' - 2(b_2P_2N - b_2'N_2) - \\
&\quad - 6(\bar{b}_2N_0P_2 - \bar{b}_2'N_{02}) - 12(\bar{b}_2N_2P_2 - \bar{b}_2'N_{12}) - 6(\bar{b}_2N_2P_2 - \bar{b}_2'N_{22}) \\
&dC_1/dt = aP_1UT - (d + k_{cat})C_1 \\
&dC_1'/dt = a'P_2UR - (d' + k_{cat}')C_1' \\
\\
&dP_3/dt = 3k_{cat}C_2 - 3(a'P_3UR - d'C_2') \\
&dC_2/dt = aP_2UT - (d + k_{cat})C_2 \\
&dC_2'/dt = a'P_3UR - (d' + k_{cat}')C_2'
\end{aligned}
$$

$$
\begin{aligned}
&dN_0/dt = (b_0P_0N - b_0'N_0) - 2(\tilde{a}N_0UT - \tilde{d}\tilde{C}_0) + 2\tilde{k}_{cat}'\tilde{C}_0' - 3(\bar{b}_0N_0P_0 - \bar{b}_0'N_{00}) - \\
&\quad - 6(\bar{b}_1N_0P_1 - \bar{b}_1'N_{01}) - 3(\bar{b}_2N_0P_2 - \bar{b}_2'N_{02}) \\
&d\tilde{C}_0/dt = \tilde{a}N_0UT - (\tilde{d} + \tilde{k}_{cat})\tilde{C}_0 \\
&d\tilde{C}_0'/dt = \tilde{a}'N_1UR - (\tilde{d}' + \tilde{k}_{cat}')\tilde{C}_0' \\
\\
&dN_1/dt = (b_1P_1N - b_1'N_1) + \tilde{k}_{cat}\tilde{C}_0 - (\tilde{a}'N_1UR - \tilde{d}'\tilde{C}_0') - (\tilde{a}N_1UT - \tilde{d}\tilde{C}_1) + \tilde{k}_{cat}'\tilde{C}_1' - \\
&\quad - 3(\bar{b}_0N_1P_0 - \bar{b}_0'N_{10}) - 6(\bar{b}_1N_1P_1 - \bar{b}_1'N_{11}) - 3(\bar{b}_2N_1P_2 - \bar{b}_2'N_{12}) \\
&d\tilde{C}_1/dt = \tilde{a}N_1UT - (\tilde{d} + \tilde{k}_{cat})\tilde{C}_1 \\
&d\tilde{C}_1'/dt = \tilde{a}'N_2UR - (\tilde{d}' + \tilde{k}_{cat}')\tilde{C}_1' \\
\\
&dN_2/dt = (b_2P_2N - b_2'N_2) + 2\tilde{k}_{cat}\tilde{C}_1 - 2(\tilde{a}'N_2UR - \tilde{d}'\tilde{C}_1') - 3(\bar{b}_0N_2P_0 - \bar{b}_0'N_{20}) - \\
&\quad - 6(\bar{b}_1N_2P_1 - \bar{b}_1'N_{21}) - 3(\bar{b}_2N_2P_2 - \bar{b}_2'N_{22})
\end{aligned}
$$

$$dN_{00}/dt = 3(\bar{b}_0 N_0 P_0 - \bar{b}'_0 N_{00}) + 2\bar{k}'_{cat} C'_{00} + 2\bar{k}'_{cat} \bar{C}'_{00} - 2(\bar{a} N_{00} UT - \bar{d} C_{00}) - 2(\bar{a} N_{00} UT - \bar{d} \bar{C}_{00})$$
$$dC_{00}/dt = \bar{a} N_{00} UT - (\bar{d} + \bar{k}_{cat}) C_{00}$$
$$dC'_{00}/dt = \bar{a}' N_{10} UR - (\bar{d}' + \bar{k}'_{cat}) C'_{00}$$
$$d\bar{C}_{00}/dt = \bar{a} N_{00} UT - (\bar{d} + \bar{k}_{cat}) \bar{C}_{00}$$
$$d\bar{C}'_{00}/dt = \bar{a}' N_{01} UR - (\bar{d}' + \bar{k}'_{cat}) \bar{C}'_{00}$$

$$dN_{01}/dt = 6(\bar{b}_1 N_0 P_1 - \bar{b}'_1 N_{01}) - 2(\bar{a} N_{01} UT - \bar{d} C_{01}) - (\bar{a} N_{01} UT - \bar{d} \bar{C}_{01}) + \bar{k}_{cat} \bar{C}_{00} + 2\bar{k}'_{cat} C'_{01} +$$
$$+ \bar{k}'_{cat} \bar{C}'_{01} - (\bar{a}' N_{01} UR - \bar{d}' \bar{C}'_{00})$$
$$dC_{01}/dt = \bar{a} N_{01} UT - (\bar{d} + \bar{k}_{cat}) C_{01}$$
$$dC'_{01}/dt = \bar{a}' N_{11} UR - (\bar{d}' + \bar{k}'_{cat}) C'_{01}$$
$$d\bar{C}_{01}/dt = \bar{a} N_{01} UT - (\bar{d} + \bar{k}_{cat}) \bar{C}_{01}$$
$$d\bar{C}'_{01}/dt = \bar{a}' N_{02} UR - (\bar{d}' + \bar{k}'_{cat}) \bar{C}'_{01}$$

$$dN_{02}/dt = 3(\bar{b}_2 N_0 P_2 - \bar{b}'_2 N_{02}) - 2(\bar{a} N_{02} UT - \bar{d} C_{02}) + 2\bar{k}_{cat} \bar{C}_{01} + 2\bar{k}'_{cat} C'_{02} -$$
$$- 2(\bar{a}' N_{02} UR - \bar{d}' \bar{C}'_{01})$$
$$dC_{02}/dt = \bar{a} N_{02} UT - (\bar{d} + \bar{k}_{cat}) C_{02}$$
$$dC'_{02}/dt = \bar{a}' N_{12} UR - (\bar{d}' + \bar{k}'_{cat}) C'_{02}$$

$$dN_{10}/dt = 3(\bar{b}_0 N_1 P_0 - \bar{b}'_0 N_{10}) - \bar{k}_{cat} C_{00} - (\bar{a} N_{10} UT - \bar{d} C_{10}) - 2(\bar{a} N_{10} UT - \bar{d} \bar{C}_{10}) + \bar{k}'_{cat} C'_{10} +$$
$$+ 2\bar{k}'_{cat} \bar{C}'_{10} - (\bar{a}' N_{10} UR - \bar{d}' \bar{C}'_{00})$$
$$dC_{10}/dt = \bar{a} N_{10} UT - (\bar{d} + \bar{k}_{cat}) C_{10}$$
$$dC'_{10}/dt = \bar{a}' N_{20} UR - (\bar{d}' + \bar{k}'_{cat}) C'_{10}$$
$$d\bar{C}_{10}/dt = \bar{a} N_{10} UT - (\bar{d} + \bar{k}_{cat}) \bar{C}_{10}$$
$$d\bar{C}'_{10}/dt = \bar{a}' N_{11} UR - (\bar{d}' + \bar{k}'_{cat}) \bar{C}'_{10}$$

$$dN_{11}/dt = 6(\bar{b}_1 N_1 P_1 - \bar{b}'_1 N_{11}) + \bar{k}_{cat} C_{01} + \bar{k}_{cat} \bar{C}_{10} - (\bar{a} N_{11} UT - \bar{d} C_{11}) - (\bar{a} N_{11} UT - \bar{d} \bar{C}_{11}) +$$
$$+ \bar{k}'_{cat} C'_{11} + \bar{k}'_{cat} \bar{C}'_{11} - (\bar{a}' N_{11} UR - \bar{d}' C'_{01}) - (\bar{a}' N_{11} UR - \bar{d}' \bar{C}'_{10})$$
$$dC_{11}/dt = \bar{a} N_{11} UT - (\bar{d} + \bar{k}_{cat}) C_{11}$$
$$dC'_{11}/dt = \bar{a}' N_{21} UR - (\bar{d}' + \bar{k}'_{cat}) C'_{11}$$
$$d\bar{C}_{11}/dt = \bar{a} N_{11} UT - (\bar{d} + \bar{k}_{cat}) \bar{C}_{11}$$
$$d\bar{C}'_{11}/dt = \bar{a}' N_{12} UR - (\bar{d}' + \bar{k}'_{cat}) \bar{C}'_{11}$$

$$dN_{12}/dt = 3(\bar{b}_2 N_1 P_2 - \bar{b}'_2 N_{12}) + \bar{k}_{cat} C_{02} + 2\bar{k}_{cat} \bar{C}_{11} - (\bar{a} N_{12} UT - \bar{d} C_{12}) + \bar{k}_{cat} C'_{12} -$$
$$- (\bar{a}' N_{12} UR - \bar{d}' C'_{02}) - 2(\bar{a}' N_{12} UR - \bar{d}' C'_{11})$$
$$dC_{12}/dt = \bar{a} N_{12} UT - (\bar{d} + \bar{k}_{cat}) C_{12}$$
$$dC'_{12}/dt = \bar{a}' N_{22} UR - (\bar{d}' + \bar{k}'_{cat}) C'_{12}$$

$$
\begin{aligned}
&dN_{20}/dt = 3(\bar{b}_0 N_2 P_0 - \bar{b}'_0 N_{20}) + 2\bar{k}_{cat} C_{10} - 2(\bar{a} N_{20} UT - \bar{d}\bar{C}_{20}) + 2\bar{k}'_{cat}\bar{C}'_{20} - \\
&\quad - 2(\bar{a}' N_{20} UR - \bar{d}' C'_{10}) \\
&d\bar{C}_{20}/dt = \bar{a} N_{20} UT - (\bar{d} + \bar{k}_{cat})\bar{C}_{20} \\
&d\bar{C}'_{20}/dt = \bar{a}' N_{21} UR - (\bar{d}' + \bar{k}'_{cat})\bar{C}'_{20}
\end{aligned}
$$

$$
\begin{aligned}
&dN_{21}/dt = 6(\bar{b}_1 N_2 P_1 - \bar{b}'_1 N_{21}) + 2\bar{k}_{cat} C_{11} + \bar{k}_{cat}\bar{C}_{20} - (\bar{a} N_{21} UT - \bar{d}\bar{C}_{21}) + \bar{k}'_{cat}\bar{C}'_{21} - \\
&\quad - 2(\bar{a}' N_{21} UR - \bar{d}' C'_{11}) - (\bar{a}' N_{21} UR - \bar{d}'\bar{C}'_{20}) \\
&d\bar{C}_{21}/dt = \bar{a} N_{21} UT - (\bar{d} + \bar{k}_{cat})\bar{C}_{21} \\
&d\bar{C}'_{21}/dt = \bar{a}' N_{22} UR - (\bar{d}' + \bar{k}'_{cat})\bar{C}'_{21}
\end{aligned}
$$

$$
\begin{aligned}
&dN_{22}/dt = 3(\bar{b}_2 N_2 P_2 - \bar{b}'_2 N_{22}) + 2\bar{k}_{cat} C_{12} + 2\bar{k}_{cat}\bar{C}_{21} - 2(\bar{a}' N_{22} UR - \bar{d}' C'_{12}) - \\
&\quad - 2(\bar{a}' N_{22} UR - \bar{d}'\bar{C}'_{21})
\end{aligned}
$$

$$
\begin{aligned}
P_0 = P_T - ((&3P_1 + 3P_2 + P_3) + (3C_0 + 3C'_0 + 6C_1 + 6C'_1 + 3C_2 + 3C'_2) + (6N_0 + 12N_1 + 6N_2) + \\
&+ 12(\tilde{C}_0 + \tilde{C}'_0 + \tilde{C}_1 + \tilde{C}'_1) + 2*9(N_{00} + 2N_{01} + N_{02} + 2N_{10} + 4N_{11} + 2N_{12} + N_{20} + 2N_{21} + \\
&+ N_{22}) + 2*18(C_{00} + C'_{00} + \bar{C}_{00} + \bar{C}'_{00} + 2C_{01} + 2C'_{01} + \bar{C}_{01} + \bar{C}'_{01} + C_{02} + C'_{02} + C_{10} + C'_{10} + \\
&+ 2\bar{C}_{10} + 2\bar{C}'_{10} + 2C_{11} + 2C'_{11} + 2\bar{C}_{11} + 2\bar{C}'_{11} + C_{12} + C'_{12} + \bar{C}_{20} + \bar{C}'_{20} + \bar{C}_{21} + \bar{C}'_{21}))
\end{aligned}
$$

$$
\begin{aligned}
UT = UT_T - ((&3C_0 + 6C_1 + 3C_2) + 12(\tilde{C}_0 + \tilde{C}_1) + 18(C_{00} + \bar{C}_{00} + 2C_{01} + 2\bar{C}_{01} + C_{02} + C_{10} + 2\bar{C}_{10} + \\
&+ 2C_{11} + 2\bar{C}_{11} + C_{12} + \bar{C}_{20} + \bar{C}_{21}))
\end{aligned}
$$

$$
\begin{aligned}
UR = UR_T - ((&3C'_0 + 6C'_1 + 3C'_2) + 12(\tilde{C}'_0 + \tilde{C}'_1) + 18(C'_{00} + \bar{C}'_{00} + 2C'_{01} + 2\bar{C}'_{01} + C'_{02} + C'_{10} + 2\bar{C}'_{10} + \\
&+ 2C'_{11} + 2\bar{C}'_{11} + C'_{12} + \bar{C}'_{20} + \bar{C}'_{21}))
\end{aligned}
$$

$$
\begin{aligned}
N = N_T - ((&6N_0 + 12N_1 + 6N_2) + 12(\tilde{C}_0 + \tilde{C}'_0 + \tilde{C}_1 + \tilde{C}'_1) + 9(N_{00} + 2N_{01} + N_{02} + 2N_{10} + \\
&+ 4N_{11} + 2N_{12} + N_{20} + 2N_{21} + N_{22}) + 18(C_{00} + C'_{00} + \bar{C}_{00} + \bar{C}'_{00} + 2C_{01} + 2C'_{01} + \bar{C}_{01} + \\
&+ \bar{C}'_{01} + C_{02} + C'_{02} + C_{10} + C'_{10} + 2\bar{C}_{10} + 2\bar{C}'_{10} + 2C_{11} + 2C'_{11} + 2\bar{C}_{11} + 2\bar{C}'_{11} + C_{12} + C'_{12} + \\
&+ \bar{C}_{20} + \bar{C}'_{20} + \bar{C}_{21} + \bar{C}'_{21}))
\end{aligned}
$$

$$
\begin{aligned}
P_{UMP} = &(3P_1 + 2*3P_2 + 3P_3) + (3C'_0 + 6C_1 + 2*6C'_1 + 2*3C_2 + 2*3C'_2) + (12N_1 + 2*6N_2) + \\
&+ 12(\tilde{C}'_0 + \tilde{C}_1 + 2\tilde{C}'_1) + (18N_{01} + 2*9N_{02} + 18N_{10} + 2*36N_{11} + 3*18N_{12} + 2*9N_{20} + \\
&+ 3*18N_{21} + 4*9N_{22}) + 18(C'_{00} + \bar{C}'_{00} + 2C_{01} + 2*2C'_{01} + \bar{C}_{01} + 2\bar{C}'_{01} + 2C_{02} + 3C'_{02} + \\
&+ C_{10} + 2C'_{10} + \bar{C}_{10} + 2\bar{C}'_{10} + 2*2C_{11} + 3*2C'_{11} + 2*2\bar{C}_{11} + 3*2\bar{C}'_{11} + 3C_{12} + 4C'_{12} + 2\bar{C}_{20} + \\
&+ 3\bar{C}'_{20} + 3\bar{C}_{21} + 4\bar{C}'_{21}))
\end{aligned}
$$

E. Supporting Information References

ref S1. Ninfa AJ, Atkinson MR (2000) PII signal transduction proteins. *Trends Microbiol*. 8:172-179.

ref S2. Ninfa AJ, Jiang P (2005) PII signal transduction proteins: sensors of α-ketoglutarate that regulate nitrogen metabolism. *Curr Opinion Microbiol.* 8:168-173.

ref S3. Atkinson MR, Kamberov ES, Weiss RL, Ninfa AJ (1994) Reversible uridylylation of the Escherichia coli PII signal transduction protein regulates its ability to stimulate the dephosphorylation of the transcription factor nitrogen regulator I (NRI or NtrC) *J. Biol. Chem*. 269:28288-28293.

ref S4. Jiang P, Ninfa AJ (2009b) Sensation and signaling of a-ketoglutarate and adenylylate energy charge by the Escherichia coli PII signal transduction protein requires cooperation of the three ligand-binding sites within the PII trimer. *Biochemistry* 48:11522:11531.

ref S5. Jiang P, Zucker P, Atkinson MR, Kamberov ES, Tirasophon W, Chandran P, Schefke BR, Ninfa AJ (1997a) Structure/function analysis of the PII signal transduction protein of *Escherichia coli*: genetic separation of interactions with receptors. *J. Bacteriol*. 179:4342-4353.

ref S6. Legewie S, Blüthgen N, Herzel H (2005) Quantitative analysis of ultrasensitive responses. *FEBS J*. 272:4071-4079.

ref S7. Gutenkunst RN, Waterfall JJ, Casey FP, Brown KS, Myers CR, Sethna JP (2007) Universally sloppy parameter sensitivities in systems biology models. *PLoS Comput Biol.* 3:1871-1878.

ref S8. Chen WW, Schoeberl B, Jasper PJ, Niepel M, Nielsen UB, Lauffenburger DA, Sorger PK (2009) Input-output behavior of ErbB signaling pathways as revealed by a mass action model trained against dynamic data. *Mol Syst Biol*. 5:239.

ref S9. Sontag ED (2002) For differential equations with r parameters, 2r+1 experiments are enough for identification. *J. Nonlinear Sci*. 12:553-583.